Journal of New Materials for Electrochemical Systems 20, 071-075 (2017)

Investigations of Electro-hydrothermally Grown ZnO Nanostructures on Copper Grids

Tzu-Yi Yu[1],Chen Hao Hung[2], Yu Shan Lee[2], Chia Feng Lin[3], Wei Min Su[2], Chien-Cheng Lu[2], Cheng-Yuan Weng[2], Yewchung Sermon Wu[4], Pei Yu Wu[4] and Hsiang Chen[2,*]

[1]Department of Information Management ,National Chi Nan University ,Taiwan, ROC
[2]Department of Applied Materials and Optoelectronic Engineering, National Chi Nan University, Taiwan, ROC
[3]Department of Materials Science and Engineering, National Chung Hsing University, Taiwan, ROC
4Department of Materials Science and Engineering, National Chiao Tung University, Taiwan, ROC

Received: October 16, 2016, Accepted: April 30, 2017, Available online: May 31, 2017

Abstract: *Two types of ZnO nanostructures were electro-hydrothermally deposited on mesh 100 and 200 copper grids. To investigate the nanostructures, multiple material analyses were used to analyze the material properties. FESEM images indicate that nanoflowers/nanorods could be grown on the mesh 100 copper grids while a single layer of ZnO nanorods could be grown on the mesh 200 copper grids. Since the size of the grid holes might influence the chemical reactions during the growth of the nanostructures, all the other material analyzes also reveale1 distinct material characteristics of these two types of nanostructures on the copper grid. Based on the experimental results, modulating the ZnO nanostructure will be helpful for future applications of ZnO nanostructures on copper substrates.*

Keywords: electro-hydrothermal, copper grids, nanoflowers, nanorods, grid holes

1. INTRODUCTION

Over the past decade, ZnO nanostructures such as nanorods [1], nanowires [2] and nanoparticles [3] have attracted growing attention because of their distinct electric, optical, and biomedical properties. Among the ZnO nanostructures, one dimensional ZnO nanorods on various substrates have been intensively studied, because the morphologies, crystalline structures, luminescence properties and antibacterial effects are strongly dependent on substrates, on which the ZnO nanorods grow. Therefore, the availability and quality of the ZnO nanorods on a certain substrate are worthy of exploration. Recently, ZnO nanorods on copper substrates have been demonstrated as solar cells [4], UV photodetectors [5], flexible piezoelectric nanogenerators [6]. In addition to the substrate, the growing method is one of the decisive factors to deposit high-quality nanorods. Based on previous reports, electrodeposition [7], vapor-phase-transport, low-temperature hydrothermal [8], chemical bath deposition methods [6] have been used to grow nanorods on top of the copper substrate. However, depositing ZnO nanorods on top of the copper grids of various sizes has not been clearly reported yet. In this research, we successfully electro-hydrothermally deposited ZnO nanorods on copper grids with two different geometric structures [9,10]. Furthermore, to characterize the nanostructures, multiple material analyses techniques including

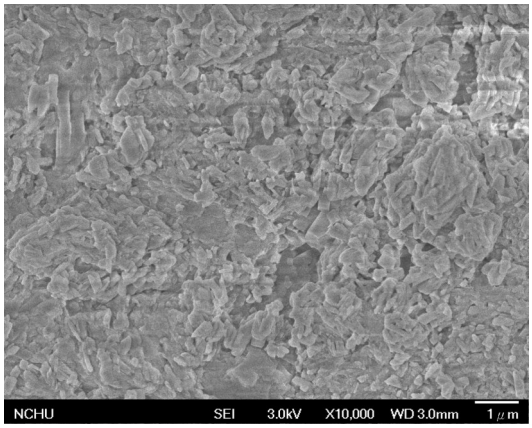

Figure 1. ZnO nanostructures on the copper grid attached to a silicon substrate. (The failure one)

*To whom correspondence should be addressed: Email: hchen@ncnu.edu.tw
Phone: +886-49-2910960; Fax: +886-49-2912238

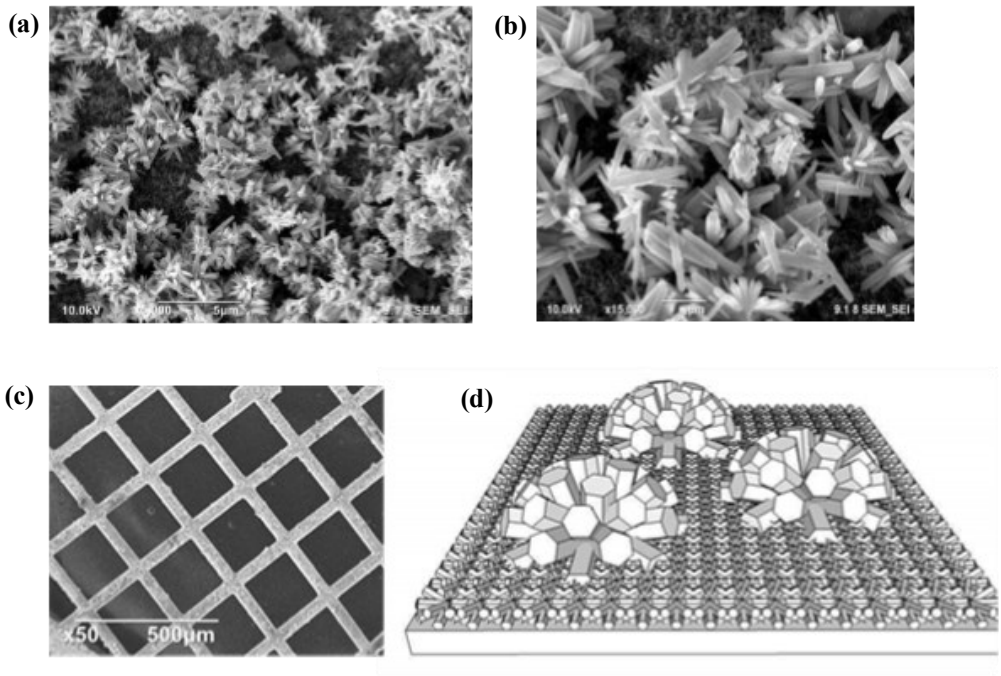

Figure 2. SEM images of (a) 5000 times magnification (b) 15000 times magnification (c) 50 times magnification for ZnO nanostructures on the mesh 100 copper grid (d) illustration of the double layer nanoflowers/nanorods structures.

field-emission scanning electron microscope (FESEM), energy dispersive X-ray spectrometry (EDX) , transmission electron microscope (TEM) and X-ray photoelectron spectroscopy (XPS)were used to study the material properties of ZnO nanorods on top of the copper grids [11,12]. Since the water flow during the growth might vary for the mesh 100 and 200 copper grids, results indicate that double-layer nanostructures can be observed for the ZnO nanostructures on the mesh 200 copper grids. On the contrary, sparsely-grown rod-clustered structures can be seen on the mesh 100 copper grids [13, 14].

To examine the surface morphologies of the two types of nanostructures, FESEM was used to view the ZnO nanorods. In addition, to analyze the element compositions, EDX was used to detect the element mapping of the nanostructures. Furthermore, to zoom in single or several nanorods on the copper grid, TEM was used to observe a single nanorod on the copper grid. Finally, XPS was used to study the chemical binding of the ZnO. Results indicate that two types of ZnO nanostructures were grown on the mesh 100 and mesh 200 copper grids. Two layers of ZnO nanostructures with ZnO nanoflowers/ZnO nanorods structures could be observed on the mesh 100 copper grids but a single layer of ZnO nanorods could be viewed on the mesh 200 copper grids. Moreover, Zn nanostructures with distinct chemical binding profiles could be measured on the two types of copper grids.

2. EXPERIMENTAL

To grow ZnO nanostructures on top of the copper grids, two types of copper grids were used (mesh 100 and mesh 200). Mesh 100 copper grids have rectangular hole density of 100 $^{\#}/_{inch^2}$ while mesh 200 have rectangular hole density of 200 $^{\#}/_{inch^2}$. The size of the grid bar for the two types of the copper grid was around 50 μm. After regular RCA clean was conducted on the copper grid, ZnO seedlayers were electrodeposited on the mesh 100 and mesh 200 copper grids for 12 sec, respectively. The electrodeposition solution was follows (potassium nitrate 2.9747g, zinc nitrate hexahydrate1.0111g and deionized water 100ml). Then, the ZnO nanostructures were hydrothermally grown on the seed layer. The hydrothermal grown solution consisted of ($C_6H_{12}N_4$ 0.98133g, $Zn(NO_3)_2$ 0.9468g and deionized water100ml). After the ZnO nanostructures were grown on the copper grid, multiple material characterizations were conducted on the nanostructures as follows. FESEM was used to observe the surface morphology and EDX was used to monitor the element compositions. Furthermore, TEM was used to study single or several ZnO nanorods on the copper grid. Finally, XPS was used to analyze the chemical binding of the ZnO nanostructures.

3. RESULT AND DISCUSSION

To grow ZnO nanostructures on the copper grids, electro-hydrothermal methods were used. After the nanostructures were grown, FESEM was used to observe the surface morphologies the ZnO nanostructures. In the beginning, the copper grid was first attached to the Si substrate. After the copper grid was electro-hydrothermally deposited with ZnO nanostructures, FESEM was used to view the surface morphology. As shown in Fig.1, failure growth and messy structures could be observed.

Instead of putting the copper grids on the Si substrate, we grew the ZnO nanostructures on the copper grid separately and directly. We electro-hydrothermally deposited ZnO nanostructure on the two types of the copper grids (mesh100 and 200) respectively.

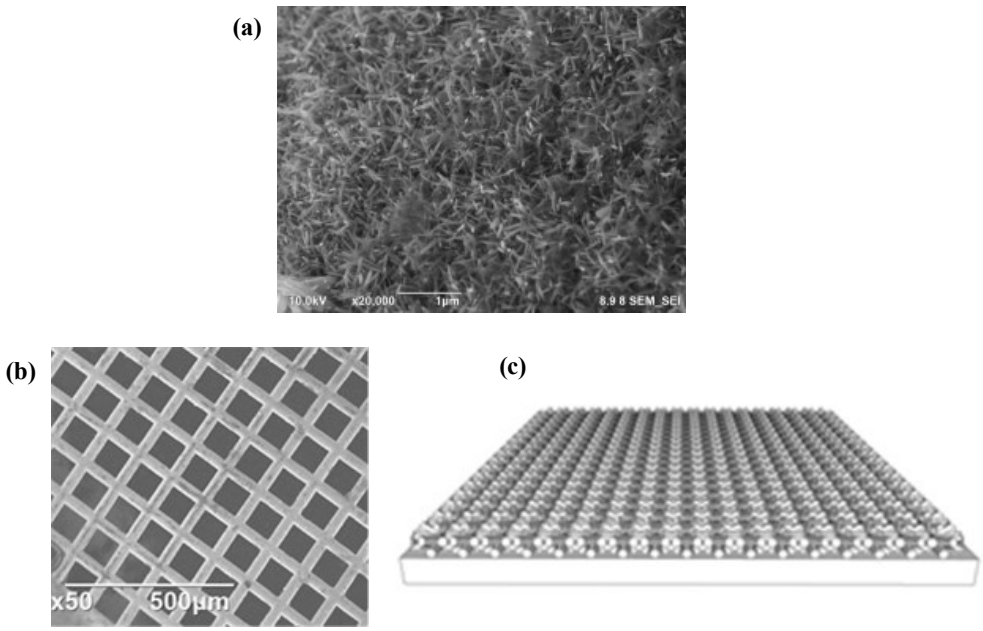

Figure 3. SEM images of (a) 25000 times magnification (b) 50 times magnification for ZnO nanostructures on the mesh 200 copper grid (c) illustration of the single layer nanorods structures.

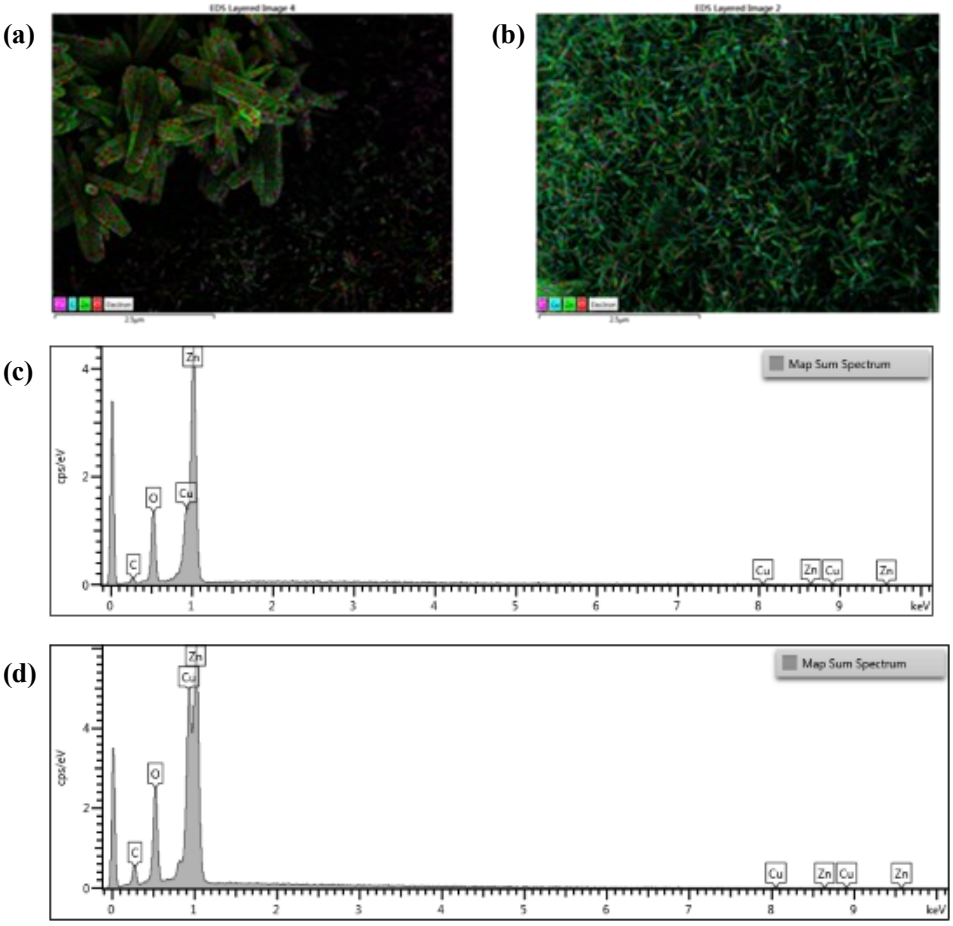

Figure 4. (a) An EDX mapping image of the double layer nanoflowers/nanorods structures on the mesh 100 copper grid (b) An EDX mapping image of the single layer nanorods structures on the mesh 200 copper grid (c) EDX spectra for (a) (d) EDX spectra for (b).

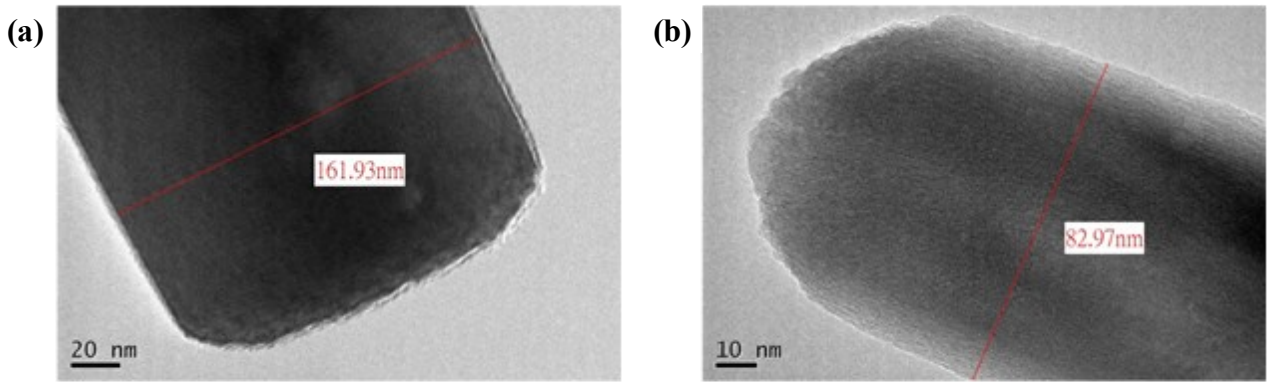

Figure 5. A TEM image for a single nanorod (a) on the mesh 100 copper gird and (b) on the mesh 200 copper gird.

FESEM images reveal that two layers of ZnO nanostructures could be observed in the mesh 100 copper grid as shown in Fig. 2 (a) and (b). Furthermore, for the image of low magnification rate as shown in Fig. 2(c), rougher or uneven surfaces appeared on the grid bars for the mesh 100 copper grids and the illustration of the double-layered structure is shown in Fig. 2 (d). On the contrary, one layer of ZnO nanorods could be seen on top of the mesh 200 copper grid as shown in Fig. 3 (a). Compared with the mesh 100 grid, more flat surfaces appeared on the grid bars for the mesh 100 copper grids as shown in Fig. 3 (b) and the illustration of the single-layered structure is shown in Fig. 3(c). The distinct nanostructures might result from the water current flow during electro-hydrothermal deposition. As for the copper grid attached on the silicon substrate, messy structures were generated because no smooth water current flow could pass through the copper grid holes. In addition, ZnO nanoflowers/nanorods structures could be grown on the mesh 100 copper grid. It might be that the rectangular holes were larger and the water current flow was not uniform. Therefore, two layers were generated. Moreover, as for the mesh 200 copper grid with smaller rectangular holes, the water current flow might be more uniform, so one layer structure was generated.

Furthermore, to examine the element compositions of these ZnO nanostructures on top of the copper grids, EDX was used to analyze the element EDX mapping and spectra. As shown in Fig. 4 (a) and (b), EDX mapping images show that Cu, Zn, O elements could be seen on ZnO nanostructures on two types of copper grids. Moreover, EDX spectrum as shown in Fig.4 (c) and (d) reveal that weaker Cu signals could be observed for the two-layerer structures on the mesh 100 copper grid while stronger Cu signals could be seen for the single layer ZnO nanorods on the mesh 200 copped grid. It might be that thicker ZnO films were on the copper grid for the two-layered structures on the mesh 100 consistent with the FESEM images.

Moreover, we used TEM to view ZnO nanorods on the side of the grid bars. Furthermore, we used TEM to examine single nanorods on the two types of copper grids. As shown in Fig. 5 (a) and (b), a large-sized single nanorod (161.93nm) could be seen on the 100 mesh grid while a smaller-sized single nanorod (82.97nm) could be seen on the 200 mesh copper grid, corresponding with the FESEM images. (Since the TEM could only observe the ZnO nanrods along the side-bar, nanoflowers on the top layer could not be observed).

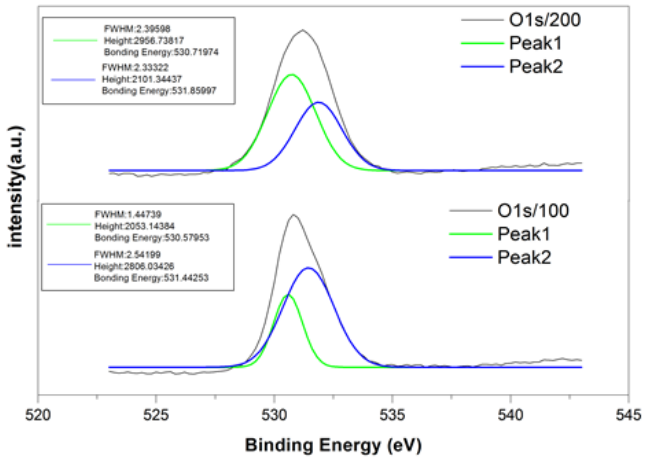

Figure 6. XPS spectra for the nanostructures on the mesh 100 and 200 copper grid.

Finally, the O1S XPS spectrum was used to study the chemical binding of the ZnO nanostructures as Fig. 6. ZnO nanostructures on the 200 mesh had stronger Zn-O-Zn (peak 1: 530.6 eV in Fig. 6) chemical binding than that on the 100 mesh, signifying. On the other hand, ZnO nanostructures on the 100 mesh had stronger Zn-O-H (peak 2: 531. 7eV in Fig. 6) chemical binding than that on the 200 mesh, while Zn-OH bonds might stand for defect-like structures [15]. Therefore, the two-layered structures on mesh 100 copper grids might have more defects than that on mesh 200 because of diversity of structures.

4. CONCLUSION

We successfully electro-hydrothermally deposited two types of ZnO nanostructures on mesh 100 and 200 copper grids. To examine the two types of nanostructures, FESEM, EDX, TEM, and XPS were used to analyze the material properties. Results indicate that nanoflowers/nanorods could be grown on the mesh 100 copper

grids while single layer ZnO nanorods could be grown on the mesh 200 copper grids. Furthermore, material analyzes also indicated different material characteristics of two types of nanostructures on the copper grid. Modulating the ZnO nanostructures in the research may be helpful for future applications of ZnO nanostructures on the copper substrate.

REFERENCES

[1] K. Yu, Y. Zhang, L. Luo, W. Wang, Z. Zhu, J. Wang, Y. Cui, H. Ma, W. Lu, Applied Physics A, 79, 443 (2004).
[2] D.-K. Kwon, S.J. Lee, J.-M. Myoung, Nanoscale, 8, 16677 (2016).
[3] H. Chen, Y.-M. Yeh, J.-Z. Chen, S.-M. Liu, B.Y. Huang, Z.-H. Wu, S.-L. Tsai, H.-W. Chang, Y.-C. Chu, C.H. Liao, Thin Solid Films, 549, 74 (2013).
[4] J. Lei, B. Yin, Y. Qiu, H. Zhang, Y. Chang, Y. Luo, Y. Zhao, J. Ji, L. Hu, RSC Advances, 5, 59458 (2015).
[5] R. Shabannia, Journal of Molecular Structure, 1118, 157 (2016).
[6] N. Sheikh, N. Afzulpurkar, M.W. Ashraf, Journal of Nanomaterials, 2013, 1 (2013).
[7] J.F. Gong, C.Y. Lan, B. Zhang, K.X. Zhang, W.H. Zhu, Advanced Materials Research, 347, 3388 (2012).
[8] Y. Lai, Y. Wang, S. Cheng, J. Yu, Journal of Electronic Materials, 43, 2676 (2014).
[9] H. Chen, Y.Y. He, M.H. Lin, S.R. Lin, T.W. Chang, C.F. Lin, C.-T.R. Yu, M.L. Sheu, C.B. Chen, Y.-S. Lin, Ceramics International, 42, 3424 (2016).
[10] H. Chen, C.B. Chen, Y.C. Chu, Ceramics International, 40, 6191 (2014).
[11] H. Wang, Q. Pan, Y. Cheng, J. Zhao, G. Yin, Electrochimica Acta, 54, 2851 (2009).
[12] H. Zhang, X. Sun, R. Wang, D. Yu, Journal of crystal growth, 269, 464 (2004).
[13] L. Podrezova, V. Cauda, S. Stassi, G. Cicero, K.A. Abdullin, B. Alpysbaeva, 49, 599 (2014).
[14] Y. Zhu, T. Yu, F. Cheong, X. Xu, C. Lim, V. Tan, J. Thong, C.H. Sow, Nanotechnology, 16, 88 (2004).
[15] L. Armelao, M. Fabrizio, S. Gialanella, F. Zordan, Thin Solid films, 394, 89 (2001).